Atomic surface occupancy of decagonal AlNiCo

S. Naidu, M. Mihalkovič,* and M. Widom
Department of Physics, Carnegie Mellon University, Pittsburgh, Pennsylvania 15213, USA
(Received 27 October 2004; revised manuscript received 11 March 2005; published 29 June 2005)

We investigate the atomic surface structure of the high temperature decagonal quasicrystalline phase of $Al_{72}Ni_{20}Co_8$ using a lattice gas Monte Carlo simulation. To avoid biasing towards a specific model we use an overdense site list with a large fraction of free sites, permitting the simulation to explore an extended region of perpendicular space. Representing the atomic surface occupancy in a basis of harmonic functions aids our analysis by directly revealing the fivefold symmetric component of our data. Patterns of occupancy are examined in both physical ("parallel") and perpendicular space, and compared with experiment in both cases. Additionally we compute the Patterson function representing correlations among atomic positions. Our results yield atomic surface structure with smooth variation of occupation and chemistry. Short distances in this model are avoided through correlations among partially occupied sites. The model naturally incorporates both an idealized average structure and intrinsic structural disorder, providing a more realistic description of the quasicrystal than is possible from an atomic surface model alone.

DOI: 10.1103/PhysRevB.71.224207 PACS number(s): 61.44.Br, 68.35.−p, 61.43.Bn

I. INTRODUCTION

AlNiCo exhibits quasicrystalline phases over a range of compositions and temperatures.[1] Of special interest is the Ni-rich quasicrystalline phase around the composition $Al_{72}Ni_{20}Co_8$. This is a decagonal phase with a period of 4.08 Å along the periodic axis, making it a simple phase relative to other members of the Al-Ni-Co family. Additionally, it appears to be most perfect structurally, even though it is stable only at high temperatures around $T=1000-1200$ K. Its structure has been extensively studied experimentally by x-ray diffraction[2,3] and electron microscopy.[4,5] Finally, since qualitatively accurate pair potentials are available,[6] structural predictions can be made based on total energy considerations.[7,8]

An idealized deterministic structure for this phase has been proposed by studying the total energy.[7] This prediction employed a multiscale simulation method, in which small system sizes were simulated starting with very limited experimental input, then rules discovered through the small scale simulations were imposed to accelerate simulations of larger-scale models. Although efficient, this approach leaves open the question of how strongly the final model was biased by the chosen method. Additionally, the Monte Carlo simulations were used for simulated annealing, attempting to identify low-energy structures, leaving open the question of a suitable description of the equilibrium quasicrystal structure at high temperatures.

We adopt a different approach here, starting from slightly different experimental input and working directly at the relevant high temperatures. The experimental input we need is (1) the density,[2] composition and temperature at which the phase exists; (2) the hyperspace positions of atomic surfaces (these are simply the positions for a Penrose tiling, with AS1 at $\nu=\pm1$ and AS2 at $\nu=\pm2$; see Fig. 1); (3) the fact that the quasicrystal is layered, with space group $10_5/mmc$, and its lattice constants (we take $a_q=6.427$ Å, and $c=4.08$ Å). The chief unknowns to be determined are the sizes, shapes and chemical occupancies of the atomic surfaces.

As in the prior study,[7] we employ Monte Carlo simulation using the same electronic-structure derived pair potentials.[6] Also, like the prior study, we employ a discrete list of allowed atomic positions. However, the prior study used sparse decorations of fundamental tiles, where the configurational freedom arose largely from flipping of the decorated tiles. Here we employ a fixed site list based on a rich decoration of fixed tiles. For a given tiling the density of allowed sites in our new simulation is much greater than the actual atomic density. The resulting atomic surface (see Fig. 1) corresponds to that of a penrose tiling with tile edge length $a_q/\tau^3=1.52$ Å (plus a few additional sites such as inside some fat rhombi). These atomic surfaces include within them the atomic surfaces previously proposed on the basis of total energy calculations,[7] and analysis of experimental data.[2,3] This larger atomic surface avoids any bias towards a particular structure solution.

The following section of this paper describes the site list and other simulation details more precisely. After that, in Sec. III we present our site occupancy both in real space and on the atomic surfaces. Our atomic surface occupancies are represented using Fourier-Bessel series, an innovation that allows us to isolate the fivefold symmetric component and filter sampling noise. We believe such a representation could prove fruitful in crystallographic structure determination as well. Indeed, previous workers[9,10] have moved beyond the polygonal atomic surface structure approximation, though they have not reached the degree of generality that we apply here.

We then compare our results with two recent experimental studies in Sec. IV. Briefly, we find broad agreement with the sizes, shapes and chemical occupancies of the atomic surfaces. A few specific points of disagreement can be addressed by relaxing our fixed site positions. Another important limitation is our consideration of just a single 4.08 Å repeat along the periodic direction.

Finally, we examine correlations among atomic positions by calculating the Patterson function and its chemically resolved partials. The Patterson function shows that short in-

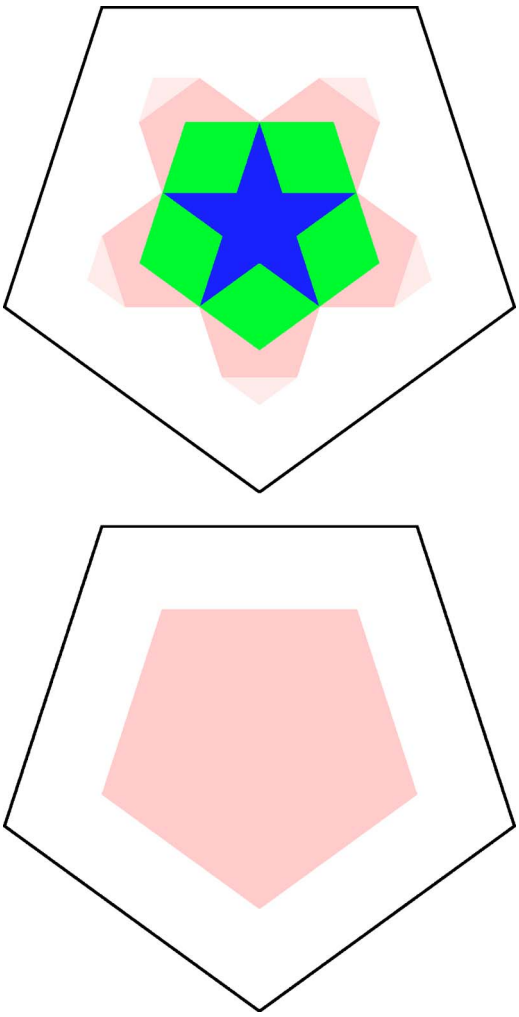

FIG. 1. (Color online) The outer pentagons illustrate the oversized atomic surface used in the present simulation. Surface AS1 ($\nu=\pm1$) on left; AS2 ($\nu=\pm2$) on right. Values of ν are the discrete perpendicular space coordinates, while the atomic surfaces are extended objects in the two continuous coordinates displayed in the figures. For comparison the ideal model proposed in Ref. 7 is inscribed inside. Color scheme: dark blue=Co; green=Ni; pink=Al; light pink=partial Al occupancy. The ideal model is slightly richer in transition metals and higher in atomic density than experiment.

teratomic distances are avoided, despite the presence of partially occupied closely spaced sites. Again, we compare our simulation with experimental results and find good agreement, although our fixed site list causes a small number of discrepancies.

Correlation functions are a necessary ingredient in a complete description of the structure because our simulated atomic surfaces exhibit partial occupancy and mixed chemical occupancy. Atomic surfaces provide a complete description of atomic positions only when their occupation is fully deterministic.

II. SIMULATION METHOD

Ideally we would perform simulations in the continuum, without any predefined site list that could bias our results.

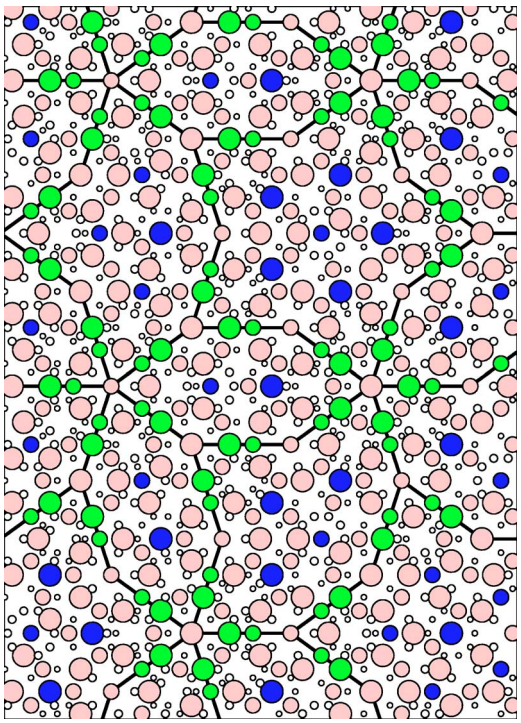

FIG. 2. (Color online) This figure illustrates our ideal tile decoration together with the excess sites (vacant) in our fixed site list. Color scheme as in Fig. 1. Small white circles indicate vacancies. Large or small atoms indicate upper or lower layer.

Unfortunately, strong binding of Al to transition metal atoms (Co and Ni, generically denoted TM) leads to phase separation into a CsCl-type of crystal plus regions of excess pure Al. Presumably this reflects a deficiency of our interatomic potentials,[6] which are not intended to be applied at a transition-metal concentration as high as the 50% which occurs in the CsCl-type crystal. This phase separation is inhibited by restricting possible atomic positions to a suitably chosen set that does not include the CsCl crystal.

Rather than specify these sites in a complex manner whose details may fail to allow some especially favorable structure, we take a realtively neutral assignment that still allows quasicrystalline structures to form. Specifically we restrict the possible atomic positions to the vertices of a Penrose lattice whose edge length is small compared to the spacing between atoms. The possible atomic sites fill space with a density 2.55 times greater than the actual atomic density, so the majority of sites are empty in any particular configuration (see Fig. 2). Our prior study of prefered structures proposed an idealized arrangement of atoms on an HBS (hexagon-boat-star) tiling of edge length a_q, as illustrated in Fig. 2.

Our Metropolis Monte Carlo simulation distributes atoms among these sites in a manner consistent with thermal equilibrium at a given temperature. We choose to focus on the temperature $T=1160$ K, which lies within the range for which the Ni-rich decagonal phase is stable[1] and has the nice property that $\beta\equiv 1/k_BT=10\ \mathrm{eV}^{-1}$.

We term this distribution of atoms among a list of discrete sites a "quasilattice gas." Within the confines of the discrete site list no further restrictions are made on configurations.

The data given below are derived from a simulation on a tiling that is a low phason strain approximant of the decagonal quasicrystal. Its lattice parameters were $159.38 \times 83.79 \times 4.08$ Å^3, it contained 9776 lattice sites and held 3838 atoms. We initially decorated the structure according to our ideal model shown in Figs. 1 and 2 (with some vacancies to achieve the desired density and composition), then brought it up to a very high temperature ($\beta = 3$ eV^{-1}, $T \approx 4000$ K) to anneal out any memory of the starting structure. At this temperature the atomic surface occupancy is nearly uniform for all chemical species. We then lowered the temperature (increased β) in a geometric series, annealing at each temperature, until we reached our data collection temperature of $T = 1160$ K and performed one final long anneal.

Each Monte Carlo step consisted of many attempted short jumps (below 3.2 Å) and long jumps (up to $a_q = 6.5$ Å) per atom. An attempted jump to an occupied site means an attempt to swap the atoms (or atom and vacancy) on the two sites. We recorded the detailed atomic site occupancy for 9000 configurations separated by sufficiently many Monte Carlo steps that the configurations can be considered as uncorrelated.

Our data analysis method differs from conventional approaches to quasicrystal atomic surface modeling. It is common to model atomic surface occupancy by breaking the atomic surface up into polygonal domains and let the occupancy be piecewise constant in each domain. This approach highlights the manner in which occupancy depends on the local real space environment, which changes discontinuously as a function in perpendicular space. Unfortunately such a piecewise continuous representation does not properly capture the effects of chemical disorder and phason fluctuations characteristic of a quasicrystal at high temperatures. Since local atomic environments constantly fluctuate, likewise the occupation preference for sites in an atomic surface domain possess certain mean values together with fluctuations.

We find the mean occupancy statistics actually vary quite smoothly over the atomic surface. To represent smoothly varying atomic surface occupancy functions we introduce a complete basis set of analytic functions and expand the occupancy in this basis. The axial symmetry of the atomic surfaces suggests using polar coordinates $(r_\perp, \theta)$. The natural function basis set for polar coordinates are combinations of cylindrical Bessel functions multiplied by complex exponentials. Thus, on a given atomic surface we express the occupancy by chemical species α as

$$\rho_\alpha(r_\perp, \theta) = \sum_{m,n} A^\alpha_{m,n} J_m(k_{m,n} r_\perp) e^{im\theta}. \quad (1)$$

The m index represents the angular mode frequency. For a given angular frequency m, the sum over n allows the representation of an arbitrary radial variation. We choose the radial frequencies $k_{m,n}$ so that all Bessel functions share a common zero at a point outside our oversized atomic surface.

To analyze our data we invert Eq. (1) to obtain the coefficients $A^\alpha_{m,n}$ using orthonormality of the basis set. We then filter out the components whose angular variation lacks fivefold symmetry (these components arise from sampling noise and from phason strains of the underlying periodic approximant) by restricting the sum over m to multiples of 5. We find it is reasonable to truncate our series at $m = n = 30$. The main features of our results are not changed by inclusion of additional terms in the series.

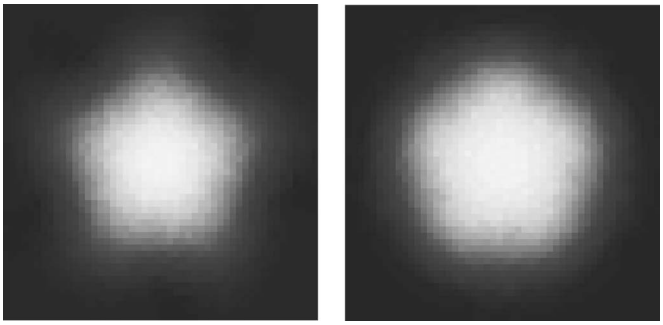

FIG. 3. This figure illustrates the filtered total occupancy of the $\nu = \pm 1$ (left) and $\nu = \pm 2$ (right) atomic surfaces. The gray scales are proportional to total atomic occupancy, scaled to the maximum for each surface. For $\nu = \pm 2$ the occupancy is almost only by Al atoms.

A. Systematic errors

Our simulation observes characteristic local structures and disorder arising from the interactions of the different chemical species and thermal fluctuations. We observe these both in parallel space occupancy and short-range correlation functions, and in perpendicular space via the atomic surface occupation statistics. Three factors limit our ability to resolve this information in perpendicular space: drift of the perpendicular space center of mass; perpendicular space resolution limited by the inverse of our approximant size; long wavelength phason fluctuations.

Local phason fluctuations such as bowtie flips[7] occur constantly during the simulation, causing the center of "gravity" (we weight each chemical species equally in calculating this) of the structure to drift in perpendicular space. Drift arises because a uniform "phason shift" of center of gravity is a Goldstone mode. As a result, thermal fluctuations of our finite size system cause random displacements of the center of gravity. To avoid smearing caused by this drift, which can obscure small scale details of the atomic surface, we recentered the perp space center of gravity for each configuration before projecting onto the Fourier-Bessel coefficients. If we had not recentered each configuration then the atomic surface occupancy functions would be substantially weaker and broader. While drift is a concern for extracting perpendicular space structure, it has no consequence for either the instantaneous structure or correlation functions in parallel space.

A second source of smearing in perpendicular space is our finite approximant size. Use of periodic approximants limits the perpendicular space structure to a collection of discrete pixels, with the pixel size inverse to the approximant lattice constants. The pixel size in Figs. 3–5 is chosen to be comparable to the resulting perpendicular space resolution. We chose our approximant sufficiently large that the pixel size is smaller than other lengths characterizing the atomic surface structure.

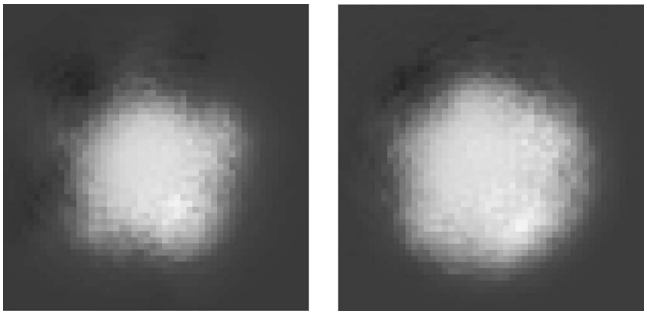

FIG. 4. This figure illustrates the unfiltered total occupancy of the $\nu = \pm 1$ (left) and $\nu = \pm 2$ (right) atomic surfaces.

The third limitation, long wavelength phason fluctuations, prevents us from improving the resolution without bound by increasing the approximant size. The reason is that our simulation of just a single 4.08 Å repeat makes the system effectively two-dimensional. Goldstone modes in two-dimensional systems create logarithmic divergences of perpendicular space flucuations (i.e., at any finite temperature the phasons are in an unlocked state[11]). For sufficiently large approximants, this would completely smear out all perpendicular space structure.

Long wavelength phason strains would not be problematic in a genuinely three-dimensional simulation, with many stacked 4.08 Å repeats because the diverging fluctuations are peculiar to two dimensions, and fluctuations are expected to be bounded in three dimensions. Unfortunately we cannot presently perform genuinely three-dimensional simulations because our restriction to an ideal site list omits the relaxed atom atomic positions that mitigate the energy cost of phason flips between adjacent 4.08 Å repeats.

Smaller approximants showed greater smearing due to the pixel size than the results illustrated here. This includes the study of approximants so small they contain just one or two tiles and hence are incapable of tile flips, and also includes approximants of intermediate size. Logarithmic divergences are so weak that if long wavelength fluctuations are unimportant for intermediate-sized approximants, they can not be

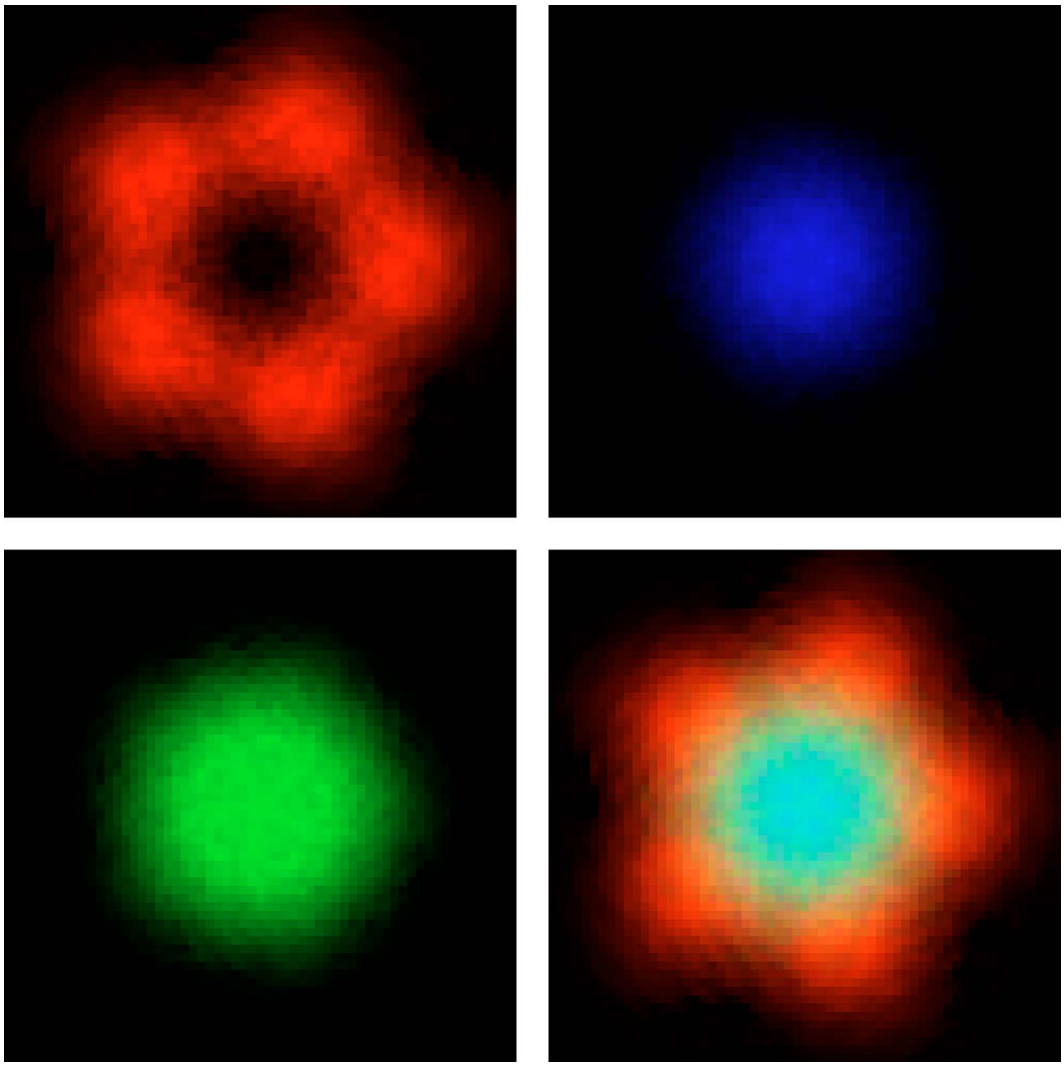

FIG. 5. (Color online) This figure illustrates the chemical occupancy of the $\nu = \pm 1$ atomic surfaces for Al, Ni, and Co atoms (respectively, red, green, and blue). The color intensities are proportional to occupancy, scaled to the maximum for each species. The rightmost figure is a false-color composite whose RGB intensities are the scaled Al, Ni, and Co occupancies.

very important for the largest size we studied.

The loss of resolution due to long wavelength phason fluctuations is therefore less than the pixel size shown. The observed smearing of the atomic surface occupancy on scales beyond the pixel size is primarily due to local phason fluctuations, which are not significantly affected by dimensionality. Local phason fluctuations also have simple descriptions in terms of chemical occupancy in parallel space. For example, a bowtie flip in our ideal model interchanges two NiNi pairs with two AlCo pairs, and is the main source of smearing on AS1 at the boundary between TM and Al occupancy.

In conclusion, provided we project only finite size samples back to perp space, we can learn a great deal about the real 3D quasicrystal structure. This includes important local structural information that is reflected in the general size, shape and chemical occupancy of the atomic surfaces, as well as a qualitative picture of the local occupation and chemical disorder which tend to broaden slightly the atomic surface distributions. We cannot learn about long-range correlations in occupancy because these are sensitive to the dimensionality of the simulation. Our paper presents only those results that are not significantly affected by dimensionality.

III. RESULTS

As in our prior[7] low temperature study, we find that the HBS tiling effectively describes the quasiperiodic layers, but the prefered chemical decoration of the tiles now becomes highly variable at certain sites. This can be described both in perpendicular and in parallel space. We discuss the structure and the disorder in perpendicular space first, then describe it in parallel space.

Figure 3 displays the average occupancy distribution on each atomic surface. The AS1 occupancy is a combination of all three chemical species. The AS2 occupancy is virtually 100% Al. The occupancies vanish well before the boundaries of our oversized atomic surfaces (coinciding roughly with the boundaries of the figures) implying that our ideal site list is more than adequately dense. No reasonable structure based on idealized sites is excluded by our discrete site list.

For comparison purposes we show the equivalent figure without filtering out the fivefold symmetry-breaking signals in Fig. 4. That is, we include all values of $m \leqslant 30$ in the sum in Eq. (1), not just multiples of 5. The filtering does not appear to qualitatively alter the figure, though it is helpful in reducing sampling noise, more clearly revealing the underlying fivefold symmetric structure that is present.

The breakdown of AS1 occupancy among Al, Ni and Co is shown in Fig. 5. A striking feature of all these occupancy plots is the smooth, continuous variation of occupancy. It is clearly not appropriate to model these densities using piecewise constant functions with polygonal boundaries, even though fivefold symmetry is present.

Ni and Co are strongly mixed with very similar distributions, concentrated at the center of AS1. Because the amount of Ni present exceeds the amount of Co, the Co occupancy vanishes more quickly than the Ni occupancy away from the center, while the Ni occupancy remains more nearly constant. In the region where the TM occupancy drops off it is largely replaced with Al so the total occupancy remains close to 100% in this crossover region.

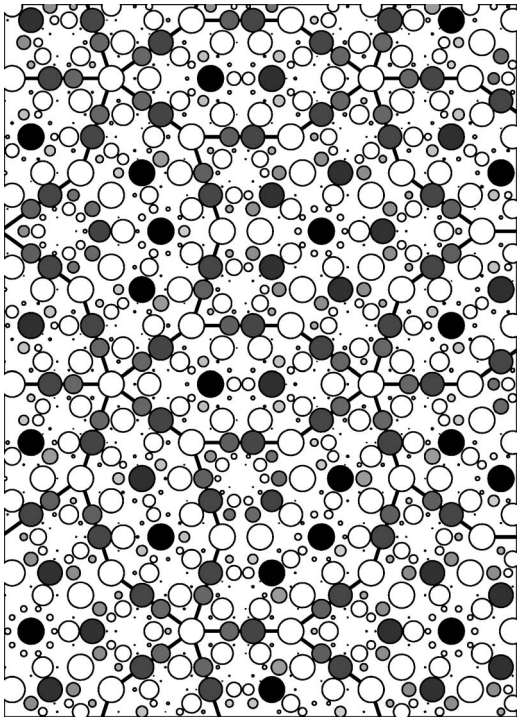

FIG. 6. Parallel space occupancy. The atomic sites are identical to Fig. 2 but the size- and color-coding differ. Here atomic size indicates total occupancy (100% = large − 0% = small) and gray scale indicates Al fraction (black = 100% TM).

In parallel space the atoms in the TM to Al crossover region occupy tile edges, and the effects of this gradient from TM to Al occupancy can be seen in Fig. 6, near tiling vertices at which two or more edges join in a ±72° angle. The pair of occupied sites on these tile edges show unequal Al/TM occupancy. The site closer to the vertex contains relatively more Al and less TM than the site further away. The site closer to the vertex in parallel space lies in the atomic surface region that is further from the center in perpendicular space. Note also that bowtie phason flips that replace TMTM pairs with AlTM pairs on tile edges are one type of excitation that replace the TM site close to a 72° vertex with an Al atom. We understand these effects energetically because the inner edge site is in a TM-rich environment. AlTM bonds are strongly favorable so this is a likely site for Al occupancy.

Despite the presence of phason fluctuations, the centers of 20 Å decagonal clusters maintain a broken symmetry center. The decagon consists of two H tiles and a B tile, and the symmetry-broken center corresponds to the sail of the B (for "sailboat") tile. Bowtie flips within the decagon tend to symmetrize the center, but the symmetrization is not complete because different sites are projected from different regions of the atomic surfaces, and the atomic surface occupancy is nonuniform. Unbounded drift would be needed to fully symmetrize the decagon center but our method does not allow this.

Far from the atomic surface centers, where the occupancy falls smoothly to zero, the atoms are mainly Al. These highly mobile atoms are in locations in parallel space where there are multiple ideal sites, too close to be simultaneously occupied, but each one with a rather similar local environment so that there is no strong energetic preference among the sites. The pair of symmetry-related sites near the center of the hexagon tile is a typical example. Other examples include rings of 10 sites surrounding the ideal Co position at the centers of boat and star tiles. These rings can hold at most three Al atoms. Jumps of Al atoms among these sites correspond to phason tile flips of the underlying very small 1.52 Å rhombus tiling.

IV. COMPARISON WITH EXPERIMENTS

We compare primarily with the refinement by Takakura.[2] We point to areas of general agreement between our results and the experimental data, then discuss the main points of disagreement.

Our simulated occupation probabilities generally agree well with experiment. The approximate sizes and shapes of our atomic surfaces agree with Takakura. We agree that AS1 contains transition metal atoms within a central region (Takakura orbit numbers[2] 1–5), separated by a fully occupied region of mixed Al/TM (orbits 6 and 7) and finally radial spokes in which Al occupancy diminishes from full to partial (orbits 8–10). We agree that AS2 (orbit numbers 11–23) contains primarily Al atoms. Takakura finds full occupancy of orbit numbers 14 and 16, but only 82% occupancy of orbit numbers 15 and 17, which are locally fairly similar (these are the Al sites adjacent to tile edge TM atoms). Our results qualitatively support this, with occupancy about 90% corresponding to orbit numbers 14 and 16, dropping to around 70–80 % for orbit numbers 15 and 17.

Now we address some interesting discrepancies between our results and experiment. Orbits number 19 and 23, localized around special points on the fringes of AS2 are fully occupied in the refinement, while we instead find partial occupancy. In parallel space these correspond to pairs of ideal sites midway between TM atoms. Partial occupancy is forced for us because the spatial separation of these ideal points (2.25 Å) is too small to allow both to be simultaneously occupied. However, if we consider multilayer structures, with $c=2\times4.08$ Å, and allow structural relaxation, we know[12] it is possible to occupy 3 out of every 4 such sites per 8.16 Å. Probably the lack of structural relaxation has caused an error in our occupancy for this orbit.

Takakura's fully occupied orbits numbers 20-22 are located on the corners of AS2. We find 60–80 % occupancy instead of full occupancy, consistently with our smoothly decreasing occupation probability. Takakura also finds a small fraction (about 20%) of TM atoms on orbits 20 and 21, while we find only Al. Perhaps the TM occupancy of orbit number 20 is related to the large atomic displacement of this orbit Takakura found during the refinement.

Surprisingly, Takakura finds partial occupancy on orbit number 11, at the very center of AS2. In parallel space this site corresponds to HBS tile vertices at which five edges meet, and is assigned occupancy 0.5. We find it is fully occupied, similar to all other HBS tile vertices. He also finds 23% TM occupancy of orbit 12, corresponding to HBS tile vertices where three tile edges meet. We find instead full Al occupancy.

It turns out that we also find a slight TM occupancy of HBS vertex sites by shifting to a slightly Al-richer composition (for example 75% Al, typical of the Al_3Co decagonal approximants). The mechanism is that NiNi pairs along HBS tile edges tend to be replaced by AlCo pairs, oriented such that the Al atoms lie close to 72° vertices.[7] In turn, these tile-edge Al atoms attract TM atoms to the vertex sites. Similarly, we obtain partial occupancy of these sites by allowing for puckering of layers, introducing an 8 Å modulation.[13] Basically, a vertex Al atom attracts Co atoms directly above and below it which must be displaced slightly away from the ideal site position because the layer spacing of $c/2=2$ Å is too short for an AlCo bond. The resulting Co displacements prevent occupancy of the remaining site (in an 8 Å period). This Co-Al-Co sequence forms the axis of a pentagonal bipyramid cluster.[13]

V. CORRELATIONS

The analysis above only presents the atomic surface occupation probabilities, but does not address correlations among the partially occupied sites. Such correlations are contained in the Patterson function, which is also known experimentally[14] and can be computed from our existing data.

Actual atomic configurations contain much more information than the atomic surface occupancies, because all correlations are reflected in the actual configurations. Figure 7 illustrates typical atomic arrangements that occur during our simulation. Comparing with the ideal model Fig. 2 reveals a great deal of disorder, including phason flips, chemical disorder and vacancies.

Among the most prominent correlations are strong anticorrelation of too-close sites. For example, the deep clefts between arms of AS1 correspond to sites that are quite close in parallel space to sites near the corners of AS2. When these AS2 sites are occupied sites within the clefts of AS1 are empty, but when these AS2 sites are empty then we find partial occupancy inside the clefts of AS1.

Another example of anticorrelation occurs because the pairs of ideal sites midway between pairs of TM atoms (e.g., Takakura orbit number 19 and 23) are too close for simultaneous occupancy. This anticorrelation arises because we used only "ideal" positions projected into parallel space from flat atomic surfaces. In reality the atomic positions are displaced somewhat away from the ideal sites, and we showed above that such displacements can have a substantial influence on occupancy statistics in cases where the ideal sites are just slightly too close together. Indeed, relaxations of our ideal structures, using either pair potentials[8,12] or full *ab initio* calculations result in displacements that are similar in many respects to those reported experimentally.[2]

A. Patterson function

Figure 8 (top) displays the Patterson function as determined experimentally from x-ray diffraction experiments.

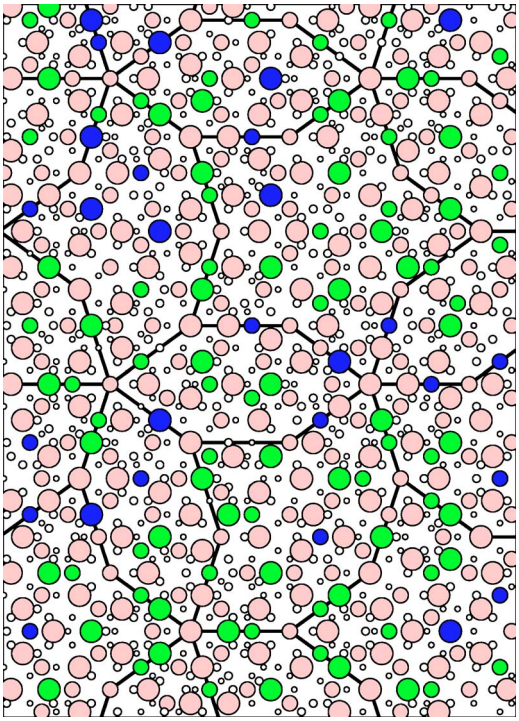

FIG. 7. (Color online) Typical atomic configuration at $T=1160$ K.

Lengths of $r_I \sim 2.43$ Å and $r_{II} \sim 2.86$ Å are typical in-plane near-neighbor distances for Al-TM and Al-Al pairs, respectively. Lengths $r_{III} \approx r_{IV} \sim 2.53$ Å are characteristic out-of-plane distances for Al-TM pairs and TM-TM pairs. Figure 8 (bottom) shows our simulated Patterson function, defined as

$$P(\mathbf{u}) = \int \rho(\mathbf{r})\rho(\mathbf{r}+\mathbf{u})d^3\mathbf{r}, \tag{2}$$

with $\rho(\mathbf{r})$ the local electron density. We calculate this function by calculating the frequency of occurrence of given pair separation vectors $\mathbf{r}$ averaged over all atoms in each of our 9000 samples. Atom pairs of species $\alpha, \beta \in (\mathrm{Al}, \mathrm{Co}, \mathrm{Ni})$ are weighted by the product of atomic numbers, $Z_\alpha Z_\beta$. We smooth the data with a Gaussian of width 0.5 Å, to approximate the impact of finite atomic size.

To analyze the result in greater detail, we present the partial Patterson functions $P_{\alpha\beta}(\mathbf{u})$, defined by replacing the electron densities ρ in Eq. (2) by the atomic densities ρ_α and ρ_β. These partials provide information that cannot be obtained directly by experiment (difference Pattersons obtained by chemical substitution can provide similar information assuming elements freely substitute). The result is shown in Fig. 9. This figure is subdivided into separate 72° domains for each atomic species pair marked. We do not include the Co-Ni pair because it is close to the average of the Co-Co and Ni-Ni pairs.

The agreement of our calculated Patterson function with experimental observation[3] (see Fig. 8) is strong in the $(x_1, x_2, 0)$ plane. Especially noteworthy is the absence of short-distance pairs, demonstrating strong anticorrelation

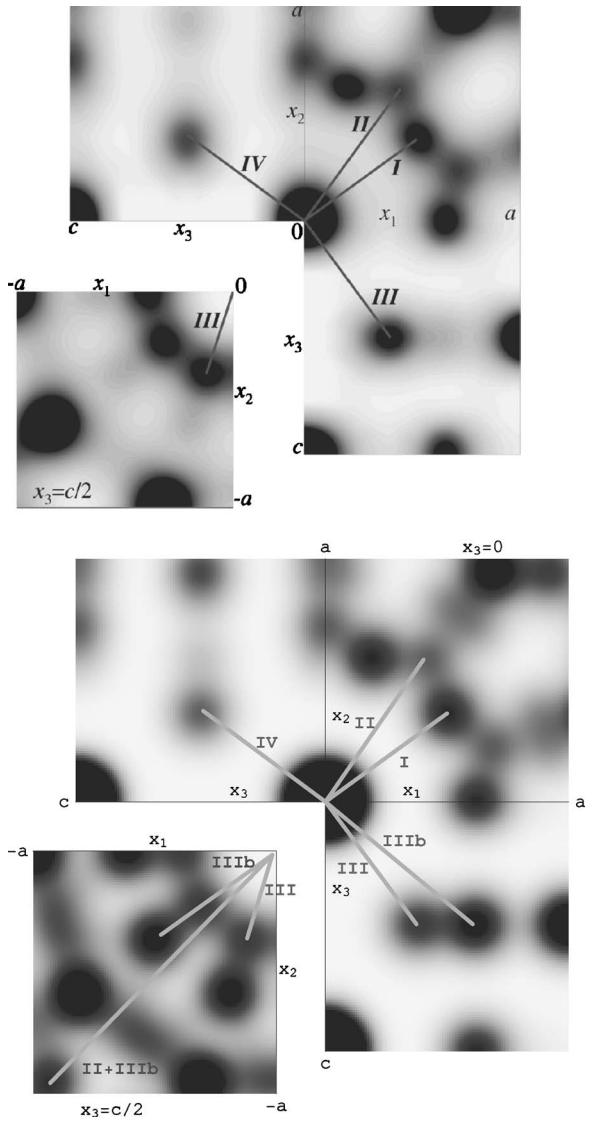

FIG. 8. (Top) Experimental Patterson function (Ref. 3). (Bottom) Simulated Patterson function. Sections shown are $(x_1, x_2, 0)$, $(x_1, 0, x_3)$, $(0, x_2, x_3)$, and $(x_1, x_2, c/2)$. Edge lengths indicated are $a \equiv a_q/\tau = 3.97$ Å and $c = 4.08$ Å.

caused by atomic repulsion. In the single-point density this simply appears as partial occupancy, with the anticorrelation not apparent.

Several important Patterson peaks are shared in common between experiment and simulation. By comparing the total Patterson functions (Fig. 8) with the partials (Fig. 9) we can identify what chemical species pairs are the main contributors to the total. The peaks located located at $(x_1, x_2, x_3) = (2.45, 0, 0)$ and symmetry equivalent r_I positions can thus be identified as Al-TM peaks. This separation occurs between Al atoms at tile vertices and TM atoms in the surrounding pentagonal ring. The peaks located at (0, 2.89, 0) and symmetry equivalent r_{II} positions are primarily due to Al-Al pairs with a slight contribution from Al-TM. This separation occurs in the Al rectangles that surround TM pairs on tile edges. Peaks at positions equivalent to $(x_1 = 0.29, x_2 = 3.78, x_3 = 0)$ are mainly Al-Al and Al-Ni. The strong peak

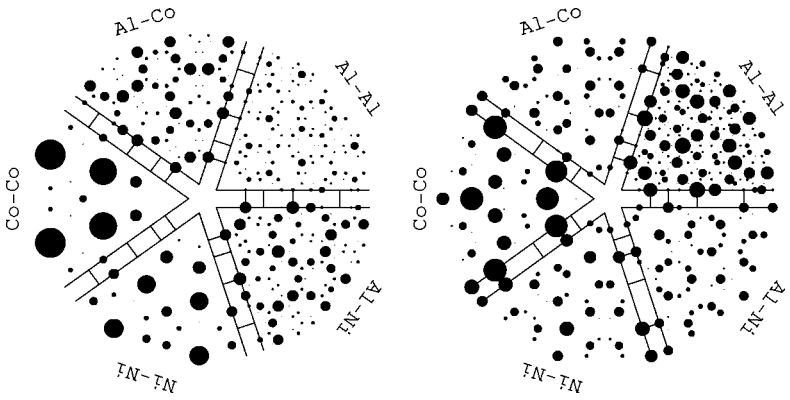

FIG. 9. Simulated partial Patterson functions. (Left) in-plane $z=0$ function; (right) out-of-plane $z=1/2$ function. Each 72° domain contains the function for the species pair indicated. Note that the origin lies at domain vertices, not at the center of the figures. Markers are placed at positions of the form $a_q/\tau^2=2.45$, $a_q/\tau=3.97$, $a_q=6.43$, and $a_q\tau=10.40$ Å away from the origin.

at $(x_1=2.89, x_2=3.78, x_3=0)$ corresponds to a predominant TM-TM in-plane separation.

In vertical sections we find the peak at the r_{III} position $(x_1,x_2,x_3)=(1.52,0,c/2)$ comes mainly from Al-TM and Ni-Ni pairs. The Ni-Ni pairs occur along tile edges. The weak peak at the r_{IV} position $(0,1.5,c/2)$ does not arise from intersection of the $(0,x_2,x_3)$ plane with any peak in the partial Patterson functions. Rather, it is the "shadow" of the peaks at positions symmetry equivalent to r_{III} [for example, $(0.47,1.45,c/2)$], which contribute to the $(0,x_2,x_3)$ plane as a result of the Gaussian smearing. The strong peak at $(x_1=3.97, x_2=0, x_3=c/2)$ occurs in all partials except Al-Al. One example of such a separation is from a tile vertex Al to a TM atom at a distance a_q/τ along a tile edge.

There are two significant points of disagreement between our results and experiment in sections taken at $x_3=c/2$. Our simulation finds strong peaks at $(x_1=2.45, x_2=0, x_3=c/2)$ and symmetry equivalent points (labeled r_{IIIb}). Inspecting the partial Patterson functions (Fig. 9) in the $z=c/2$ layer we see these peaks are caused mainly by Al-Al pairs. Such a separation occurs between a tile vertex Al and an Al in the surrounding pentagonal ring in an adjacent layer. The other significant disagreement occurs at $(x_1=3.72, x_2=3.78, x_3=c/2)$ and symmetry equivalent points. These two points differ by a displacement of type r_{II}, so we label it as $r_{II}+r_{IIIb}$. Owing to closure of the Patterson peaks under addition, the presence of either one demands the presence of the other. r_{IIIb} points are visible strongly in the $(x_1,x_2,c/2)$ section but more weakly in the $(0,x_2,x_3)$ section because it is displaced off the $x_1=0$ plane. Inspecting the partial Patterson functions, we see again these peaks are caused by Al-Al correlations. The strong correlations and high Al concentration allow these pairs to contribute strongly to the total Patterson function, despite their weak scattering $[\sim(Z_{Al}=13)^2]$.

We are not certain what causes these strong peaks to occur in our simulation but apparently not in experiment. The leading possibilities are (1) our fixed site lists maintain flat layers and 4 Å periodicity, while Cervellino's experimental sample apparently exhibits puckering leading to an 8 Å modulation; (2) weak Al-Al bonds exhibit more variation of length than is permitted by our fixed site simulation. The first explanation agrees with the fact that the extra peaks occur only at $x_3=c/2$. The second explanation agrees with the fact that the peaks are caused entirely by Al-Al pairs. Indeed, it is known that some pentagonal ring Al atoms undergo significant displacement when relaxed, provided that a breaking of the 4 Å stacking periodicity is allowed.[15]

Returning our attention to the partial Patterson functions in Fig. 9, we notice other interesting facts. Focus first on the $z=0$ layer. A dramatic difference between the Al-X correlations (X=Al, Co or Ni) and the TM-TM correlations is the relative absence of short distance separations in TM-TM. This reflects the strength of Al-TM bonding, which, together with the low TM concentration causes TM atoms to be surrounded only by Al so far as possible. The strongest Al-Al correlations occur at 2.88 and 4.66 Å which are, respectively, edges and chords of the small Al pentagons surrounding each HBS vertex. The strongest short Al-TM peak at 2.45 Å corresponds to the distance from HBS vertices to the mixed Al/TM pentagons. In general, we see oscillations in the mean values of the partials as a function of distance from the origin, which match the Friedel oscillations of the interatomic pair potentials.

The strong peaks in the Co-Co correlation function at separations 4.67, 7.56, and 12.22 Å are caused by the strong preference of Co to occupy isolated sites in tile interiors. Rigidity of the tiles then leads to very long-range Co correlations within individual tiles and between neighboring tiles.

At $z=1/2$ the strongest Al-Al peak occurs at 6.43 Å horizontal separation, corresponding to the HBS tile edge length. This arises in the $z=1/2$ layer due to height alternation of the vertices, essentially revealing the two-level nature of the tiling. The shortest distance peaks in the TM-TM correlations occur at horizontal separation of 1.52 Å (total separation of 2.54 Å). This length is the separation of adjacent TM sites on tile edges. It is stronger in the Ni-Ni pair than in Co-Co because tile edges prefer the Ni-Ni decoration. However, replacement of Ni-Ni tile edge pairs with Al-Co or Al-Ni[7] is evident in the peaks at the same position in the Al-TM partials.

VI. CONCLUSION

In conclusion, we used Monte Carlo simulation of a quasilattice gas to predict the single point occupancy and two-point correlation functions of Al-Co-Ni in the "basic" Ni-rich decagonal quasicrystal phase. First-principles-derived interatomic potentials provide a highly realistic description of structural energies. Our fixed site approach employs an oversized atomic surface model to avoid biasing the

results in favor of any particular tile or cluster decorations. Unlike x-ray diffraction experiments, which cannot distinguish between Co and Ni atoms, we obtain complete information about chemical occupancy.

We find the single point occupancy statistics correspond to fairly simple atomic surface structures that are generally consistent with experimental observation. Both total occupancy and chemical content vary smoothly across the atomic surfaces. We employ a basis of Fourier-Bessel functions to represent our atomic surface occupancy, which is more naturally suited to smooth atomic surfaces than the conventional decomposition into piecewise constant occupation subdomains.

Because atomic surfaces are not sharply faceted, short distances occur between partially occupied sites. Short interatomic separations are avoided in reality as a result of pair correlations among partially occupied sites. Such a description of the quasicrystal structure is a significant improvement over one relying on atomic surfaces alone, which require sharp faceting and intricate structure to avoid short separations. Our pair correlation functions are in general agreement with experimental Patterson functions.

Certain disagreements between theory and experiment were found, most of which we believe are caused by our fixed-site approach which neglects small relaxation of atomic positions. This approximation alters the occupancy of certain sites and overstates the strength of correlations among Al atoms. Future study of site occupancy thus requires that sites be allowed small displacements from their ideal positions. In particular, it is necessary to allow for an 8 Å modulation of the basic 4 Å periodic structure. Extending the model to multiple 4 Å layers will have the added benefit of giving more nearly three-dimensional behavior and thus more realistic phason fluctuations.

ACKNOWLEDGMENTS

We wish to acknowledge useful discussions with C. L. Henley. This work was supported in part by NSF Grant No. DMR-0111198.

*Also at Institute of Physics, Slovak Academy of Sciences, 84228 Bratislava, Slovakia.

[1] S. Ritsch, C. Beeli, H.-U. Nissen, T. Godecke, M. Scheffer, and R. Luck, Philos. Mag. Lett. **78**, 67 (1998).
[2] H. Takakura, A. Yamamoto, and A.-P. Tsai, Acta Crystallogr., Sect. A: Found. Crystallogr. **57**, 576 (2001).
[3] A. Cervellino, T. Haibach, and W. Steurer, Acta Crystallogr., Sect. B: Struct. Sci. **58**, 8 (2002).
[4] E. Abe, K. Saitoh, H. Takakura, A.-P. Tsai, P. Steinhardt, and H.-C. Jeong, Phys. Rev. Lett. **84**, 4609 (2000).
[5] Y. Yan, S. J. Pennycook, and A.-P. Tsai, Phys. Rev. Lett. **81**, 5145 (1998).
[6] I. Al-Lehyani, M. Widom, Y. Wang, N. Moghadam, G. M. Stocks, and J. A. Moriarty, Phys. Rev. B **64**, 075109 (2001).
[7] M. Mihalkovič, I. Al-Lehyani, E. Cockayne, C. L. Henley, N. Moghadam, J. A. Moriarty, Y. Wang, and M. Widom, Phys. Rev. B **65**, 104205 (2002).
[8] F. Gahler (unpublished).
[9] L. Elcoro, J. M. Perez-Mato, and G. Madaraiga, Acta Crystallogr., Sect. A: Found. Crystallogr. **50**, 182 (1994).
[10] M. V. Jaric and S.-Y. Qiu, Phys. Rev. B **49**, 6614 (1994).
[11] L.-H. Tang and M. V. Jaric, Phys. Rev. B **41**, 4524 (1990).
[12] C. L. Henley, M. Mihalkovič, and M. Widom, J. Alloys Compd. **342**, 221 (2002).
[13] E. Cockayne and M. Widom, Philos. Mag. A **77**, 593 (1998).
[14] W. Steurer, T. Haibach, B. Zhang, S. Kek, and R. Luck, Acta Crystallogr., Sect. B: Struct. Sci. **49**, 661 (1993).
[15] M. Mihalkovič, C. L. Henley, and M. Widom, J. Non-Cryst. Solids **334&335**, 177 (2004).